Stochasticity of metabolism and growth at the single-cell level

Daniel J. Kiviet[†*#~], Philippe Nghe[†#$], Noreen Walker[#], Sarah Boulineau[#], Vanda Sunderlikova[#] & Sander J. Tans[*#]
† equally contributing authors
* corresponding authors
# FOM institute AMOLF, Science Park 104, 1098 XG Amsterdam, the Netherlands.
~ Department of Environmental Systems Science, ETH Zurich, and Department of Environmental Microbiology, Eawag, Switzerland
$ current address: Laboratoire de Biochimie, UMR 8231 CNRS/ESPCI, École Supérieure de Physique et de Chimie industrielles, 10 rue Vauquelin, 75005 Paris, France

Elucidating the role of molecular stochasticity[1] in cellular growth is central to understanding phenotypic heterogeneity[2] and the stability of cellular proliferation[3]. The inherent stochasticity of metabolic reaction events[4] should have negligible effect, because of averaging over the many reaction events contributing to growth. Indeed, metabolism and growth are often considered to be constant for fixed conditions[5,6]. Stochastic fluctuations in the expression level[1,7-9] of metabolic enzymes could produce variations in the reactions they catalyze. However, whether such molecular fluctuations can affect growth is unclear, given the various stabilizing regulatory mechanisms[10-12], the slow adjustment of key cellular components such as ribosomes[13,14], and the secretion[15] and buffering[16,17] of excess metabolites. Here, we used time-lapse microscopy to measure fluctuations in the instantaneous growth rate of single *E. coli* cells, and quantified time-resolved cross-correlations with the expression of *lac* genes and enzymes in central metabolism. We show that expression fluctuations of catabolically active enzymes can propagate and cause growth fluctuations, with transmission depending on the limitation of the enzyme to growth. Conversely, growth fluctuations propagate back to perturb expression. Accordingly, enzymes were found to transmit noise to other unrelated genes *via* growth. Homeostasis is promoted by a noise-cancelling mechanism that exploits fluctuations in the dilution of proteins by cell-volume expansion. The results indicate that molecular noise is propagated not only by regulatory proteins[18,19] but also by metabolic reactions. They also suggest that cellular metabolism is inherently stochastic, and a generic source of phenotypic heterogeneity.

To investigate the dynamics of cellular growth, we followed individual *Escherichia coli* cells growing on different nutrients. Among them was the synthetic sugar lactulose[20], which is imported and catabolized by the LacY and LacZ enzymes like its analog lactose, but unlike lactose does not induce *lac* operon expression (Fig. 1a). Mixtures of lactulose and the gratuitous inducer IPTG thus allowed us to vary the mean *lac* expression level independently and hence to explore different regimes of noise transmission. We determined the instantaneous growth rate $\mu(t)$ of individual cells within microcolonies at sub-cell-cycle resolution for various growth conditions, using time-lapse microscopy[19] at high acquisition rates and automated image analysis (Supplementary Information). We found that $\mu(t)$ varied significantly in time, both within one cell-cycle and between different cell-cycles (Fig. 1b-c, Extended Data Fig. 1), with noise intensities (standard deviation over the mean) ranging between 0.2 and 0.4 (Fig. 1d). Consistently, the growth rates of sister cells were significantly correlated (Extended Data Fig. 2). We found that the typical timescales of the fluctuations were somewhat smaller than the mean cellular doubling time, as quantified by the autocorrelation functions $R_{\mu\mu}(\tau)$ (Fig. 1e-f). Such a scaling with doubling time is typical for protein concentration fluctuations[21]. Thus, the data indicated randomly fluctuating growth limitations, and suggested they could be caused by concentration fluctuations of cellular components.

To study the relation between growth and *lac* enzymes, we quantified the fluctuations in the *lac* production rate $p(t)$ and concentration $E(t)$ using GFP labeling (Fig. 1a, g-i and Extended Data Fig. 1). We computed the cross-correlation functions $R_{p\mu}(\tau)$ and $R_{E\mu}(\tau)$, which indicate whether expression fluctuations correlate with μ-fluctuations occurring time τ later, and thus inform on the direction of transmission[9,22]. Both $R_{p\mu}(\tau)$ and $R_{E\mu}(\tau)$ showed positive correlations regardless of the IPTG concentration (Fig. 2a, e-g). Their shapes and symmetries did depend on IPTG however. At low and intermediate IPTG, $R_{E\mu}(\tau)$ was nearly symmetric around τ=0 while $R_{p\mu}(\tau)$ was asymmetric with larger weight at $\tau > 0$ (Fig. 2e-f and Extended Data Fig. 3). This would indicate that p fluctuations on average correlated more strongly with μ fluctuations that occur later. Such a delay in μ is consistent

with the idea that *lac* expression fluctuations produce variations in lactulose catabolism, which in turn propagate through the metabolic network and perturb growth.

At high IPTG $R_{E\mu}(\tau)$ displayed a positive peak at $\tau < 0$ (Fig. 2g and Extended Data Fig. 3). Thus, E fluctuations correlated more strongly with μ fluctuations occurring *earlier*, which suggested backward transmission from growth to expression. Such a growth-to-expression coupling could be caused by specific regulatory interactions[13,23,24], or more generally by growth fluctuations that cause variations in general components that are required for transcription and translation. Overall, the data suggested that noise not only propagated forward, from expression to growth, but also backward, from growth to expression.

To determine whether back-and-forth transmission could explain the correlations we developed a stochastic model. A black-box approach was followed, in which noise propagation is represented by phenomenological transmission coefficients that do not specify molecular details (Fig. 2b). Despite the circulating noise, the system could be decomposed into distinct noise transmission modes; here termed the *lac* catabolism, common noise, and dilution modes (Fig. 2d). The cross-correlation curves for all induction levels (Fig. 2e-g) were fitted jointly, using the transmission strength from the common noise source to p as a single free parameter (Fig. 2h-j).

The effects of induction could be explained by altered intensities of the modes. At low and intermediate IPTG, the *lac* catabolism mode was dominant, with *lac* noise causing up to 30% of the growth noise (Extended Data Table 1). At higher IPTG this mode weakened because of decreased transmission from E to μ. This decrease is plausible, as catalyzed reactions are less dependent on catalyst when the latter is abundant, consistent with the observed relation between the mean $\overline{E}$ and $\overline{\mu}$ (Fig. 2c). On the other hand, the rather constant $R_{p\mu}(0)$ (Fig. 2e-g) indicated that the common-noise mode had an almost fixed intensity for all IPTG concentrations. To further probe the generality

of this mode we made a number of genetic modifications. We found that it remained active when we knocked-out the *lac* repressor, changed the GFP position within the operon, altered the type of fluorescent protein, or used an exogenous constitutive promoter (Extended Data Fig. 4a-d). These data suggest that common noise transmits to expression in general, which does not exclude additional coupling by specific regulatory interactions.

Next, we tested key findings. First, if the asymmetry in $R_{p\mu}(\tau)$ (Fig. 2e-f) is indeed caused by *lac* catabolism, this asymmetry should be suppressed when carbon enters central metabolism via another pathway. Growth on acetate was similarly slow as on lactulose and low induction, but $R_{p\mu}(\tau)$ was now indeed nearly symmetric (Fig. 3a-b, Extended Data Fig. 3). At the same time, $R_{E\mu}(\tau)$ became more asymmetric as predicted for a dominant common noise mode transmission (Fig. 3a-b, Extended Data Fig. 3). When growing on other natural substrates including lactose, the $R_{E\mu}$ peak-width scaled roughly with doubling time consistent with dilution setting the transmission delay timescales (Fig. 3b, Extended Data Fig. 5). To test further whether *lac* fluctuations could be causal in the growth noise, we exposed the cells to IPTG pulses in a microfluidic device. The resulting pulses in *lac* expression were indeed followed by a pulse in growth (Extended Data Fig. 6a). Next, we aimed to mimic common noise fluctuations by growing cells on glucose minimal medium and pulsing with amino acids. These pulses indeed produced transient increases in μ and p (Extended Data Fig. 6b), consistent with common noise propagating to enzyme expression and to growth.

Second, the network structure implied a homeostatic control mechanism: upward fluctuations in common noise *increase* E when transmitted via p, but also *decrease* E when transmitted via μ (Fig. 2b). These opposing effects offer a direct prediction: if the positive pathway dominates, $R_{E\mu}(\tau)$ should be positive, as is the case so far. If the negative pathway would dominate however, $R_{E\mu}(\tau)$ should become negative (Fig. 3c). One cannot manipulate how volume changes affect dilution. To tilt the balance, we thus looked for constructs with a weaker coupling to common noise in the positive

pathway, as measured by $R_{p\mu}(0)$. A constitutively expressed mCherry with a two-fold lower $R_{p^*\mu}(0)$ indeed displayed negative $R_{E^*\mu}(\tau)$ (Fig. 3d and Extended Data Fig. 3). Thus, two parallel antagonistic pathways that together form a so-called incoherent feed-forward network motif[25] can partially cancel noise. This cancelling also explains why $R_{E\mu}(0)$ is low even though $R_{p\mu}(0)$ is high at high induction where common noise dominates (Fig. 2g). Interestingly, while up-fluctuations in μ are associated with up-fluctuations in E (Fig. 2g), increases in mean $\overline{\mu}$ lead to *decreases* in $\overline{E}$ (Extended Data Fig. 5e)[13,23]. These opposing dependencies suggest that different mechanisms underlie these two types of expression variations.

Third, if *lac* enzymes transmit to growth and growth transmits to expression in general, then *lac* enzymes ought to transmit also to other genes. Hence we quantified $p^*(t)$ of mCherry controlled by promoters with no known functional interactions with the *lac* system. For lactulose and low induction, mCherry fluctuations indeed occurred after *lac* fluctuations on average (Fig. 3f, Extended Data Fig. 7a-b) in accordance with predictions (Fig. 3e). In contrast, this delay was absent for acetate, which is consistent because *lac* then does not transmit to growth (Extended Data Fig. 7c-d). Noise in *lac* expression can thus couple to other genes without specific regulatory interactions.

For the *lac* genes, the *lac* catabolism mode transmitted to growth only when the mean *lac* expression was kept artificially low and limited the mean growth rate. Hence, we wondered whether limiting enzymes in central metabolism could similarly perturb growth. For growth on lactose, glycolysis is considered limited by *pfkA*, and the TCA cycle by *icd* but not by *gltA*, while in acetate, *gltA* is limiting, *icd* may be limiting, but *pfkA* is not[26-28]. We indeed observed positive time delays in $R_{p\mu}$ for *pfkA* and *icd* in lactose, and for *gltA* and *icd* in acetate, but not in the other cases (Fig. 3g, Extended Data Fig. 7e). This pattern of correlation delays is consistent with the mechanism found for *lac*, in which growth limitation in steady-state resulted in noise transmission to growth. Notably, the differences in noise transmission behavior were observed for enzymes catalyzing nearby reactions in the pathway.

For instance, *icd* acts almost directly after *gltA*, but *icd* displayed delayed correlation in lactose while *gltA* did not. This excludes the possibility that the delayed correlations are caused by synchronous fluctuations of *pfkA*, *gltA*, *icd*, and other central metabolic genes. Together, the results indicate that expression-to-growth noise propagation occurs more generally for limiting genes.

Our study shows that fluctuations in gene expression can affect the growth stability of a cell, and in turn, growth noise affects gene expression. This entanglement between growth and expression noise reflects the inherent auto-catalytic nature of self-replicating systems: metabolic enzymes help synthesize the building blocks for their own synthesis. The results raise the question how different fluctuating metabolic activities within the cell are coordinated, and which regulatory mechanisms are implicated in maintaining growth homeostasis. Metabolic stochasticity could allow clonal cells in a population to adopt a wide spectrum of metabolic states, and hence enable bet-hedging strategies to optimally exploit new conditions. Metabolic stochasticity could represent a generic source of cellular heterogeneity[29], but also prevent optimal growth[30] and limit efficient biosynthesis. Novel approaches are required to incorporate noise transmission within the current theoretical framework of metabolism.

Supplementary Information is available in the online version of the paper.

Acknowledgments Work in the laboratory of S.J.T. is part of the research program of the Stichting voor Fundamenteel Onderzoek der Materie (FOM), which is financially supported by the Nederlandse Organisatie voor Wetenschappelijke Onderzoek (NWO). D.J.K. was partly supported by an ETHZ Postdoctoral Fellowship. We thank Tom Shimizu, Jeroen van Zon, Huib Bakker, Kobus Kuipers, Martin Ackermann, Pieter-Rein ten Wolde, Matthias Heinemann, and members of the Tans group for critical reading of the manuscript.

Author Contributions D.J.K. and S.J.T. conceived and designed the experimental approach. D.J.K., P.N., N.W., V.S. and S.B. performed the experiments. P.N. developed the theoretical model. D.J.K., P.N., and S.J.T. wrote the manuscript.

Author Information Reprints and permissions information is available at www.nature.com/reprints. The authors declare no competing financial interests. Correspondence and requests for materials should be addressed to S.J.T (tans@amolf.nl) or D.J.K (kiviet@env.ethz.ch).

References:

1 Wilkinson, D. J. Stochastic modelling for quantitative description of heterogeneous biological systems. *Nat Rev Genet* **10**, 122-133 (2009).

2 Eldar, A. & Elowitz, M. B. Functional roles for noise in genetic circuits. *Nature* **467**, 167-173 (2010).

3 Heiden, M. G. V., Cantley, L. C. & Thompson, C. B. Understanding the Warburg Effect: The Metabolic Requirements of Cell Proliferation. *Science* **324**, 1029-1033 (2009).

4 Lu, H. P., Xun, L. Y. & Xie, X. S. Single-molecule enzymatic dynamics. *Science* **282**, 1877-1882 (1998).

5 Fell, D. *Understanding the control of metabolism*. (Portland, 1997).

6 Herrgard, M. J., Covert, M. W. & Palsson, B. O. Reconstruction of microbial transcriptional regulatory networks. *Curr Opin Biotechnol* **15**, 70-77 (2004).

7 Elowitz, M. B., Levine, A. J., Siggia, E. D. & Swain, P. S. Stochastic gene expression in a single cell. *Science* **297**, 1183-1186 (2002).

8 Ferguson, M. L. *et al.* Reconciling molecular regulatory mechanisms with noise patterns of bacterial metabolic promoters in induced and repressed states. *Proceedings of the National Academy of Sciences of the United States of America* **109**, 155-160 (2012).

9 Munsky, B., Neuert, G. & van Oudenaarden, A. Using Gene Expression Noise to Understand Gene Regulation. *Science* **336**, 183-187 (2012).

10 Neidhardt, F. C., Ingraham, J. L. & Schaechter, M. *Physiology of the bacterial cell : a molecular approach*. (Sinauer Associates, 1990).

11 Rodriguez, M., Good, T. A., Wales, M. E., Hua, J. P. & Wild, J. R. Modeling allosteric regulation of de novo pyrimidine biosynthesis in Escherichia coli. *Journal of theoretical biology* **234**, 299-310 (2005).

12 Hart, Y. *et al.* Robust Control of Nitrogen Assimilation by a Bifunctional Enzyme in E. coli. *Mol Cell* **41**, 117-127 (2011).

13 Klumpp, S., Zhang, Z. & Hwa, T. Growth rate-dependent global effects on gene expression in bacteria. *Cell* **139**, 1366-1375 (2009).

14 Yun, H. S., Hong, J. & Lim, H. C. Regulation of ribosome synthesis in Escherichia coli: effects of temperature and dilution rate changes. *Biotechnol Bioeng* **52**, 615-624 (1996).

15 el-Mansi, E. M. & Holms, W. H. Control of carbon flux to acetate excretion during growth of Escherichia coli in batch and continuous cultures. *Journal of general microbiology* **135**, 2875-2883 (1989).

16 Wilson, W. A. *et al.* Regulation of glycogen metabolism in yeast and bacteria. *FEMS microbiology reviews* **34**, 952-985 (2010).

17 Levine, E. & Hwa, T. Stochastic fluctuations in metabolic pathways. *Proceedings of the National Academy of Sciences of the United States of America* **104**, 9224-9229 (2007).

18 Pedraza, J. M. & van Oudenaarden, A. Noise propagation in gene networks. *Science* **307**, 1965-1969 (2005).

19 Rosenfeld, N., Young, J. W., Alon, U., Swain, P. S. & Elowitz, M. B. Gene regulation at the single-cell level. *Science* **307**, 1962-1965 (2005).

20 Dean, A. M. A molecular investigation of genotype by environment interactions. *Genetics* **139**, 19-33 (1995).

21 Austin, D. W. *et al.* Gene network shaping of inherent noise spectra. *Nature* **439**, 608-611 (2006).

22 Dunlop, M. J., Cox, R. S., 3rd, Levine, J. H., Murray, R. M. & Elowitz, M. B. Regulatory activity revealed by dynamic correlations in gene expression noise. *Nature genetics* **40**, 1493-1498 (2008).

23 Scott, M., Gunderson, C. W., Mateescu, E. M., Zhang, Z. & Hwa, T. Interdependence of cell growth and gene expression: origins and consequences. *Science* **330**, 1099-1102 (2010).

24 Goerke, B. & Stulke, J. Carbon catabolite repression in bacteria: many ways to make the most out of nutrients. *Nat Rev Microbiol* **6**, 613-624 (2008).
25 Shen-Orr, S. S., Milo, R., Mangan, S. & Alon, U. Network motifs in the transcriptional regulation network of Escherichia coli. *Nature genetics* **31**, 64-68 (2002).
26 Walsh, K. & Koshland, D. E., Jr. Characterization of rate-controlling steps in vivo by use of an adjustable expression vector. *Proc Natl Acad Sci U S A* **82**, 3577-3581 (1985).
27 Wagner, A. *et al.* Computational evaluation of cellular metabolic costs successfully predicts genes whose expression is deleterious. *Proceedings of the National Academy of Sciences of the United States of America* **110**, 19166-19171 (2013).
28 Oh, M. K., Rohlin, L., Kao, K. C. & Liao, J. C. Global expression profiling of acetate-grown Escherichia coli. *J Biol Chem* **277**, 13175-13183 (2002).
29 Balazsi, G., van Oudenaarden, A. & Collins, J. J. Cellular decision making and biological noise: from microbes to mammals. *Cell* **144**, 910-925 (2011).
30 Wang, Z. & Zhang, J. Impact of gene expression noise on organismal fitness and the efficacy of natural selection. *Proceedings of the National Academy of Sciences of the United States of America* **108**, E67-76 (2011).

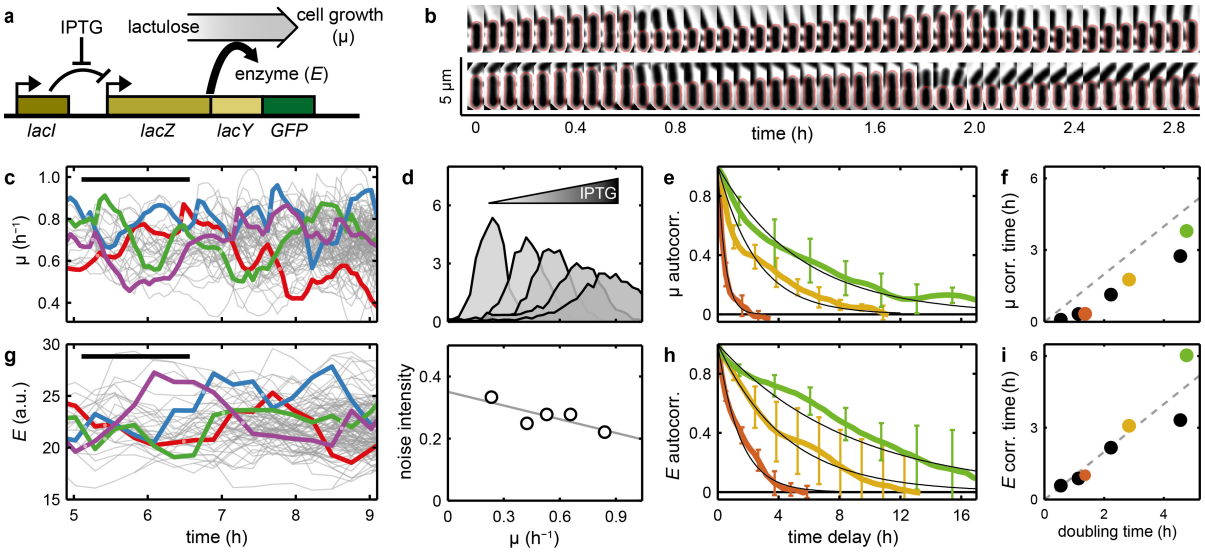

Fig. 1. Growth rate variability in single *E. coli* cells. a, Schematic diagram of the studied system. Lactulose is metabolized by the *lac* enzymes, but does not induce *lac* expression. Mean *lac* expression can hence be varied independently by the inducer IPTG. GFP is fused transcriptionally in the *lac* operon (Extended Data Table 2). **b,** Aligned phase contrast images for two lineages. Microcolonies were grown on polyacryl pads (0.1% lactulose and 200 μM IPTG) for 8 to 9 generations. Up to 48 images were taken per hour. Red line: cell boundary from image analysis. **c,** Instantaneous growth rate $\mu(t)$ against time, determined by fitting exponentials to the cellular length. Four lineages are colored for clarity. Black bar: mean division time. Light points: division events. **d,** Top: Histograms of μ values for different IPTG levels. Bottom: Noise intensity (standard deviation over the mean). **e,** Autocorrelation function of $\mu(t)$ for low (4 μM, green), intermediate (6 μM, ochre), and high (200 μM, brown) IPTG levels. For clarity, error bars denoting the standard deviation are indicated only for a fraction of the points. Black lines: exponential fits that provide the correlation time. Correlation functions were determined along the branched lineages (Extended Data Fig. 8). **f,** $\mu(t)$ correlation time versus mean doubling time. Colors are as in e, black points are for growth on defined rich, lactose, succinate, and acetate (in order of increasing doubling time). **g-i,** as

panels c, e, and f, but for the fluorescence intensity reporting for $E(t)$ within single cells. Protein concentrations were determined by the mean fluorescence per unit area (Extended Data Fig. 1e-g).

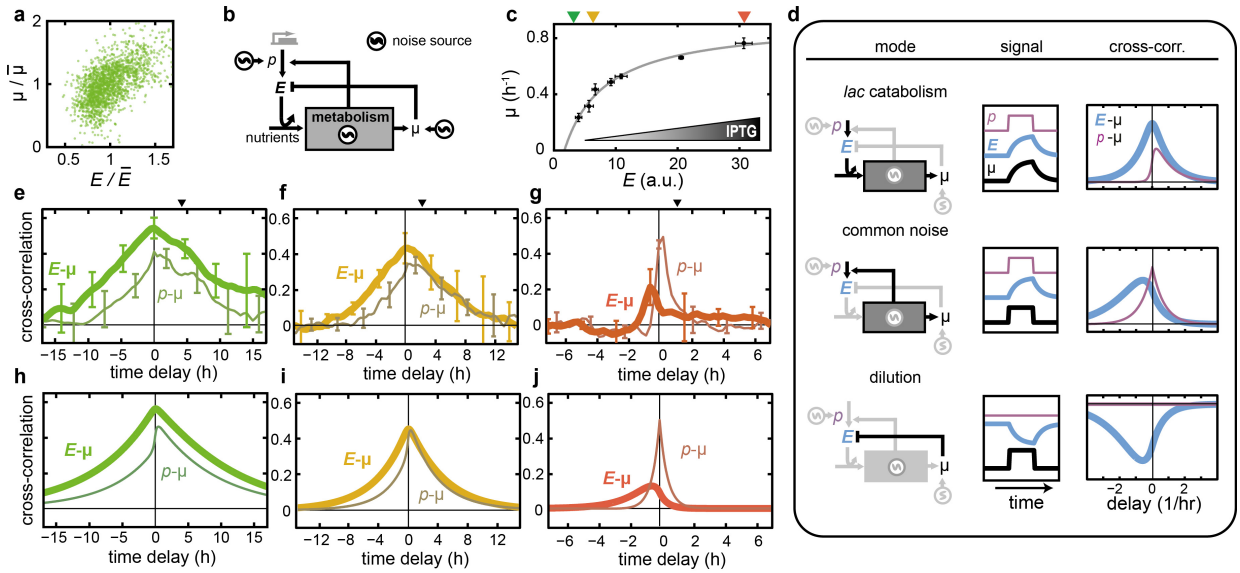

Fig. 2 Cross-correlation functions and mathematical model. a, Instantaneous growth rate against *lac* enzyme concentration from one microcolony, corresponding to the cross-correlation value $R_{E\mu}(0)$ in panel e. **b,** Model of the coupling between expression and growth noise. Two noise sources are specific to p and μ, one is common to p and μ. Correlations arise when noise emitted from one source is received by two observables (p, E, or μ). Analytical solutions revealed all contributing pathways, and showed they were finite despite the looped network structure (Supplementary Information). **c,** The mean growth rate versus the mean expression level, as measured for different levels of IPTG induction. Line: fit to a Monod growth model. **d,** Three classes of noise transmission modes. As an example, a noise source (left) emits a block wave, giving rise to signals μ, p, and E (middle) and their cross-correlations (right). Other pathways contribute as well. For instance, common noise can also drive the catabolism mode. **e-g,** Cross-correlation functions $R_{p\mu}(\tau)$ for the enzyme production rate $p(t)$ and growth rate $\mu(t)$ (thin line), as well as $R_{E\mu}(\tau)$ for the enzyme concentration $E(t)$ and $\mu(t)$ (thick line). Growth is on lactulose (0.1 %) with IPTG: 4 μM (e), 6 μM (f),

200 μM (g). Top triangles indicate mean division time. Error bars denoting the standard deviation are indicated for some data points only. The main features were robust to changing the growth determination method and taking the cell width into account (Extended Data Fig. 4e-h). Growth and expression differences typically did not correlate with location within the microcolony (Extended Data Fig. 4i). Protein production rates were determined by the time-derivative of the total fluorescence per cell (Extended Data Fig. 1e-h). **h-j,** Fits to the experimental data (panels e-f).

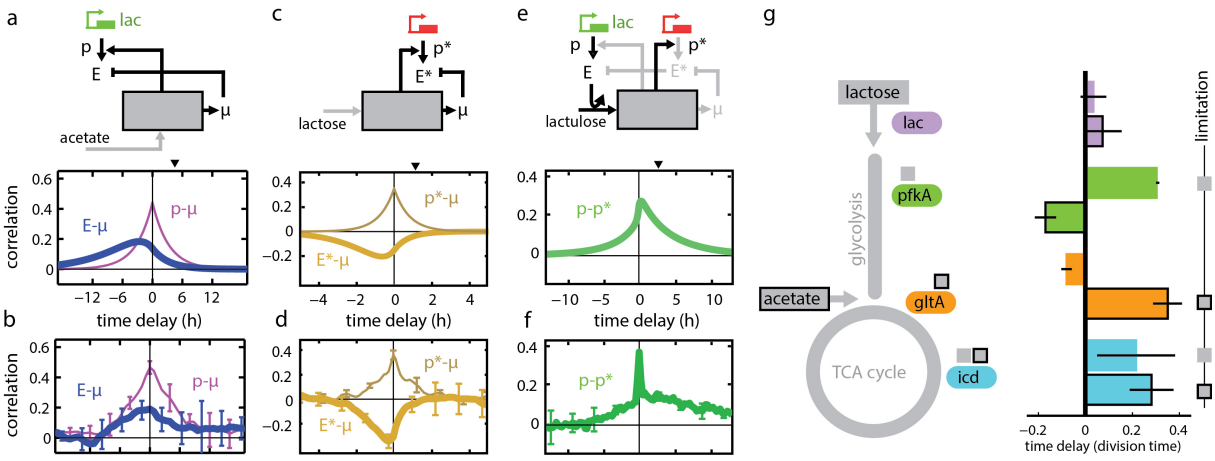

Fig. 3 Model predictions and experimental tests. Top: re-wired noise transmission networks with predicted dominant pathways (black). Colored genes indicate labeling with GFP and mCherry. Middle: predicted cross-correlation with mean doubling time (triangle). Bottom: measured cross-correlation. **a-b,** For growth on acetate the *lac* enzymes are catabolically inactive. **c-d,** Gene with a weaker coupling from common noise to expression (compared to the *lac* operon), leading to dominant dilution. **e-f,** Transmission from the *lac* genes to another gene *via* growth. When the *lac* genes do not transmit because cells grow on acetate, the correlation is symmetric (Extended Data Fig. 7c-d). **g**, Time delays for *lac*, *pfkA*, *gltA*, and *icd* in lactose (not boxed) and acetate media (boxed), as derived from the correlation functions $R_{p\mu}(\tau)$ (Extended Data Fig. 7e). Small square boxes indicate which gene is considered limiting in steady-state in a particular medium (see main text).